

6  
K-75

106

Laboratory of Nuclear Problems

S.M. Korenchenko

and

V.G. Zinov

EXPERIMENTAL INVESTIGATION OF THE ELASTIC AND INELASTIC  
INTERACTION OF  $\pi$ -MESONS WITH HYDROGEN IN THE ENERGY REGION

300-370 MeV\*

*International conf. of mesons and  
Recently Discovered Particles, Padova-  
Venice, September, 1957, 8 p 23.*

1957

---

\* The results of this experiment were reported at the  
International Conference on Mesons and Recently Discovered Particles  
/September, 1957, Padova-Venice/.

Laboratory of Nuclear Problems

S.M. Korenchenko

and

V.G. Zinov

EXPERIMENTAL INVESTIGATION OF THE ELASTIC AND INELASTIC  
INTERACTION OF  $\pi^-$ -MESONS WITH HYDROGEN IN THE ENERGY REGION  
300-370 MeV\*

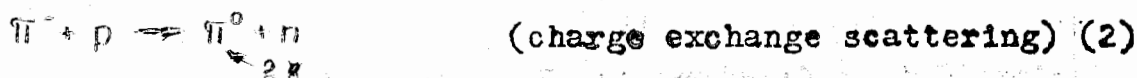
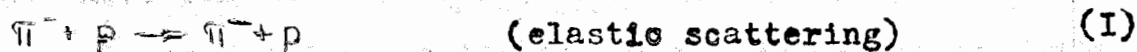
Объединенный институт  
ядерных исследований  
БИБЛИОТЕКА

1957

---

\* The results of this experiment were reported at the  
International Conference on Mesons and Recently Discovered Particles  
/September, 1957, Padova- Venice/.

The present paper is devoted to the study of  $\pi^-$ -meson interaction with hydrogen in the energy region 300-370 MeV. At these energies besides the scattering processes



pion production in pion-proton collisions may take place:



We have measured the differential cross-sections of processes (1) and (2) at the energies of the incident  $\pi^-$ -meson beam 307 and 333 and the differential cross sections for the production at  $80^\circ$  laboratory angle of charged meson in the processes (3) and (4) at the energies of 307, 333 and 370 MeV.

### P i o n   b e a m s

Pion beams with the energy of 250, 307, 333 and 370 MeV obtained at the synchrocyclotron of the Joint Institute for Nuclear Research (Fig. 1)<sup>1,2</sup> have been used. Pi-minus mesons generated in Be target inside the synchrocyclotron chamber traversed the collimator mounted in the synchrocyclotron magnet yoke, were deflected by a focusing magnet on the hydrogen target. The energy of  $\pi^-$ -meson beams was determined from a range measurement in copper. A typical range curve is given in Fig. 2. The muon fraction in the beams was about  $5 \pm 1,5\%$ . The pion intensities which used are: were at the energy of 250 MeV = 45 mesons.cm<sup>2</sup>.sec<sup>-1</sup>, 307 MeV = 100-150 mesons.cm<sup>2</sup>.sec<sup>-1</sup>; 333 MeV = 80-100 mesons.cm<sup>2</sup>.

$\text{sec}^{-1}$ , 370 MeV - 45 mesons.  $\text{cm}^{-2}$ .  $\text{sec}^{-1}$ .

The intensity distribution across the beam has been studied for every energy using the scintillator 1 x 1 x 1 cm.

### Scintillation Counters and Electronic Equipment

Scintillation counters (Fig. 3 and 5) have been used for detecting the particles. Counters 1, 3, 4, 5, 6, 7, 8 are plexiglas cells filled with terphenyl solution in phenylcyclohexane (3g/liter). Counter N 1 has the size 6 x 6 x 1 cm, counters N 3, 4, 5, 6 and 7 - 12, 6 x 11, 5 x 1 cm, counter N 8 - 16 x 17 x 1, 5 cm. Counter N 2 was made of a tholane crystal 6 x 6 x 0, 4 cm to reduce the background of scattered mesons. Counters N 1, 2, 3, 5, 7 and 8 were connected with photomultipliers by means of light pipes made of plexiglas. Counters N 4 and N 6 were connected with photomultipliers by means of hollow light pipes with mirror aluminium walls. The necessity for the use of hollow light pipes was due to the fact that the light pipes made of plexiglas are sensitive to high velocity charged particles (true, with an efficiency of only 5%, apparently, due to Cerenkov radiation).

The photomultipliers have been placed into a double magnetic screen to protect them from the synchrocyclotron fringing magnetic field. Impulses from the photomultipliers were applied to the forming device and then were fed into a multichannel coincidence circuit through ~80 m long coaxial cables. A block-diagram of electronic equipment is shown in Fig. 4. Germanium detector fast coincidence circuits were used. These circuits make it possible to obtain resolving times. up to  $0,5 \cdot 10^{-8}$  sec with a sensitivity of ~0,5 volts. The fast anticoincidence circuit was also made of germanium detec-

tors and had a resolving time of  $\sim 2,2 \cdot 10^{-8}$  sec. Tube-made slow coincidence and anticoincidence circuits ( $\tau \sim 5 \cdot 10^{-7}$  sec) worked with standard formed pulses going from the output of the fast coincidence circuits.

The efficiency of coincidence and anticoincidence circuits has been verified by mounting the corresponding counters in one line along the  $\pi$ -meson beam, at reduced intensity. The efficiency of coincidence circuits was close to 100%, the efficiency of fast anticoincidence circuits was not less than 97%; the efficiency of slow anticoincidence circuits was not less than 99,9%.

#### Liquid Hydrogen Target

Liquid hydrogen was put into a duraluminium cylinder placed into a styrofoam vessel. The walls of the cylinder in the working region are  $\sim 0,1$  mm thick. The diameter of it in the working region is 11 cm. The quantity of hydrogen on the beam range was on the average  $0,735$  g/cm<sup>2</sup>, the quantity of the material of target walls  $\sim 0,35$  g/cm<sup>2</sup>.

#### Elastic Scattering of Negative Pions

The elastic scattering geometry is given in Fig. 3. The double coincidence of counters 1 and 2 served as a monitor. The scattered pions have been detected by telescopes, consisting of the counters 3,4 and 5,6 (more exactly, quadruple coincidences of counters 1,2,3,4 and 1,2,5,6 were measured). To reduce the background from accidental coincidences 1,2,3,4, events of the last type were counted in anticoincidence with counter 7.

The observations were made at the angles of  $30^\circ$ ,  $45^\circ$ ,  $60^\circ$ ,  $80^\circ$ ,  $100^\circ$ ,  $125^\circ$  and  $150^\circ$  in the laboratory system. In the measurements at the angle of  $30^\circ$ ,  $45^\circ$  and  $60^\circ$  aluminium absorbers were placed before the counters 4 and 6 to remove the recoil protons. At the incident pion energy 307 MeV this absorbers were 28,4; 20,2; 9,4 g/cm thick respectively and 31,0; 21,6; 10,8 g/cm<sup>2</sup> - at the energy 333 MeV. In the measurement at other angles the aluminium absorbers 5,4 g/cm<sup>2</sup> thick were placed before counters 4 and 6 to reduce the accidental coincidence background. The influence of aluminium absorbers of different thickness on the efficiency of pions detection has been investigated experimentally.

Several measurement runs have been conducted for every energy of  $\pi^-$ -meson beam. The ratios of the numbers of quadruple coincidences observed in one of the runs of measurements /  $E_{\pi^-} = 307$  MeV/ to those of double coincidences ( Q/D) are given in Table I.

The ratios Q/D observed at the energy of 333 MeV were similar to those presented in Table I. The differential cross section has been calculated by the formula

$$\left(\frac{d\sigma}{d\omega}\right)_{\pi^- \rightarrow \pi^-} = \frac{(Q/D)_{\text{with H}} - (Q/D)_{\text{without H}}}{K \cdot N \cdot \omega} \quad (6)$$

Table I

$E_{\pi} = 307 \text{ MeV}$        $\pi^- + p \rightarrow \pi^- + p$

| Laboratory angles                           | 30°             | 45°            | 60°            | 80°            | 100°            | 125°           | 152°           |
|---|-----------------|----------------|----------------|----------------|-----------------|----------------|----------------|
| Solid angle subtended by telescope (sterad) | 0,034           | 0,0413         | 0,0413         | 0,0512         | 0,0512          | 0,0512         | 0,0494         |
| $Q/D \cdot 10^6$ with hydrogen              | $111,2 \pm 3,0$ | $63,6 \pm 1,6$ | $41,5 \pm 1,4$ | $25,9 \pm 0,9$ | $20,9 \pm 0,75$ | $23,5 \pm 1,2$ | $30,0 \pm 1,1$ |
| $Q/D \cdot 10^6$ without hydrogen           | $81,7 \pm 2,4$  | $34,0 \pm 1,6$ | $23,0 \pm 1,1$ | $12,8 \pm 0,6$ | $9,2 \pm 0,7$   | $10,9 \pm 1,0$ | $18,6 \pm 0,7$ |
| The difference                              | $29,5 \pm 3,9$  | $29,6 \pm 2,3$ | $18,5 \pm 1,8$ | $13,1 \pm 1,1$ | $11,7 \pm 1,0$  | $12,7 \pm 1,6$ | $11,4 \pm 1,3$ |

Table II

$E_{\pi} = 307 \pm 9 \text{ MeV}$        $\pi^- + p \rightarrow \pi^- + p$

| The angle in c.m.s.  | 41,3°           | 60,6°           | 78,5°           | 100,0°            | 119,0°          | 140,0°          | 160,3°          |
|--|-----------------|-----------------|-----------------|-------------------|-----------------|-----------------|-----------------|
| Differential cross section of elastic scattering in $10^{-27} \text{ cm}^2 \text{ sterad.}^{-1}$ | $1,30 \pm 0,16$ | $1,06 \pm 0,13$ | $0,76 \pm 0,09$ | $0,500 \pm 0,032$ | $0,63 \pm 0,07$ | $0,92 \pm 0,10$ | $1,17 \pm 0,13$ |

where  $N = 0,443 \cdot 10^{24}$  - the average number of hydrogen atoms per  $1 \text{ cm}^2$ ,  $\omega$  - the solid angle subtended by telescopes,  $K$  - a coefficient taking into account conventional corrections for such effects: decrease of telescope efficiency due to aluminium absorber, increase of the count due to the  $\gamma$ -ray conversion from  $\pi^0$ -mesons in counters N 3 and N 5, muon contamination of the beam, meson absorption in the target walls and in counters N 2,3,5, counting losses in the scaler of the monitor and some other corrections.

Measurements which we shall speak about below have shown that at energies of  $\pi^-$ -mesons larger than 300 MeV the effect of meson production by mesons becomes observable. Corrections for this effect have been made by assuming that the produced mesons in the centre of mass system are distributed isotropically and their energetic spectrum has a trapezium form.

The values of the differential cross section of elastic scattering in c.m. system obtained after all the corrections have been made are given in Tables 2 and 3 and in Fig. 6 and 7.

Expressing by the least square method the differential cross section dependence on the centre mass scattering angle as a spherical harmonics sum:

$$\frac{d\sigma}{d\omega} = A + B P_1(\cos \vartheta) + C P_2(\cos \vartheta) \tag{7}$$

$$\frac{d\sigma}{d\omega} = A + B P_1(\cos \vartheta) + C P_2(\cos \vartheta) + D P_3(\cos \vartheta) + E P_4(\cos \vartheta) \tag{8}$$

where  $P_k$  - is the  $k$ 'th spherical harmonic, we obtained the values of the coefficients (in  $10^{-27} \text{ cm/sterad}^{-1}$ ) given in Tables 4 and 5. In the last column of Tables 4 and 5 are ~~the~~ given <sup>the</sup> corresponding values of the weighted least squares sums.

$$M = \sum_{i=1}^7 (\Delta_i / \epsilon_i)^2, \tag{9}$$



where  $\Delta_1$  - the deviation of the calculated value of the differential cross section from the experimental.  $\xi_1$  - the experimental error in the measured differential cross section. It can be seen from Tables 4 and 5 that the accuracy of the performed calculations does not make it possible on the basis of the angular distribution form to draw a definite conclusion on the necessity of taking into account the D-wave contribution to elastic scattering.

The cross section of the process (I) obtained when integrating (7) is equal

for  $E_{\pi^-} = 307 \text{ MeV}$   $\sigma_{\pi^+ \pi^-} = (11,1 \pm 0,6) 10^{-27} \text{ cm}^2$   
 for  $E_{\pi^-} = 333 \text{ MeV}$   $\sigma_{\pi^+ \pi^-} = (10,7 \pm 0,6) 10^{-27} \text{ cm}^2$

Table 4

$E_{\pi^-} = 307 \text{ MeV}$

| $A_{-}$         | $B_{-}$         | $C_{-}$         | $D_{-}$          | $E_{-}$          | $M_{-}$ |
|-----------------|-----------------|-----------------|------------------|------------------|---------|
| $0,88 \pm 0,05$ | $0,34 \pm 0,09$ | $0,65 \pm 0,09$ | -                | -                | 3,22    |
| $0,85 \pm 0,05$ | $0,21 \pm 0,09$ | $0,43 \pm 0,15$ | $-0,24 \pm 0,15$ | $-0,18 \pm 0,13$ | 0,75    |

Table 5

$E_{\pi^-} = 333 \text{ MeV}$

| $A_{-}$         | $B_{-}$         | $C_{-}$         | $D_{-}$          | $E_{-}$           | $M$  |
|-----------------|-----------------|-----------------|------------------|-------------------|------|
| $0,85 \pm 0,05$ | $0,35 \pm 0,09$ | $0,60 \pm 0,09$ | -                | -                 | 4,13 |
| $0,83 \pm 0,05$ | $0,29 \pm 0,12$ | $0,51 \pm 0,16$ | $-0,11 \pm 0,15$ | $-0,054 \pm 0,16$ | 3,76 |

$E_{\pi^-} = 333 \pm 9$  Mev

$\pi^- + p \rightarrow \pi^- + p$

Angle in the c.m.s.      41,9°      61,3°      79,2°      100,8°      119,7°      140,6°      159,2°

Differential cross section of elastic scattering in  $10^{-27} \text{ cm}^2/\text{sterad}^{-1}$

|  |                       |                      |        |        |        |
|--|-----------------------|----------------------|--------|--------|--------|
|  | 1,28 ± 0,14           | 0,91 ± 0,69 ± 0,51 ± | 0,52 ± | 0,96 ± | 0,93 ± |
|  | ± 0,10 ± 0,09 ± 0,032 | ± 0,07 ± 0,10 ± 0,13 |        |        |        |

Table 6

$E_{\pi^-} = 307$  Mev

$\pi^- + p \rightarrow \pi^0 + n$

Angle in the laboratory system      15°      30°      45°      60°      80°      112,5°      135°      152°

The solid angle subtended by telescope (sterad)

|  |       |       |       |       |       |       |       |        |
|--|-------|-------|-------|-------|-------|-------|-------|--------|
|  | 0,012 | 0,036 | 0,044 | 0,055 | 0,055 | 0,055 | 0,055 | 0,0414 |
|--|-------|-------|-------|-------|-------|-------|-------|--------|

Q/D x  $10^6$  with hydrogen

|  |            |             |              |              |              |              |              |              |
|--|------------|-------------|--------------|--------------|--------------|--------------|--------------|--------------|
|  | 80,0 ± 3,4 | 160,0 ± 6,0 | ± 95,4 ± 4,1 | ± 64,9 ± 2,9 | ± 39,7 ± 1,7 | ± 30,3 ± 1,3 | ± 34,6 ± 1,5 | ± 22,3 ± 1,0 |
|--|------------|-------------|--------------|--------------|--------------|--------------|--------------|--------------|

Q/D x  $10^6$  without hydrogen

|  |            |              |              |              |              |              |              |              |
|--|------------|--------------|--------------|--------------|--------------|--------------|--------------|--------------|
|  | 22,6 ± 1,9 | ± 26,8 ± 2,7 | ± 21,9 ± 2,0 | ± 22,3 ± 1,8 | ± 18,0 ± 1,2 | ± 16,0 ± 1,1 | ± 23,0 ± 1,2 | ± 13,2 ± 0,9 |
|--|------------|--------------|--------------|--------------|--------------|--------------|--------------|--------------|

The differences

|  |            |               |              |              |              |              |              |             |
|--|------------|---------------|--------------|--------------|--------------|--------------|--------------|-------------|
|  | 57,4 ± 3,9 | ± 133,2 ± 6,6 | ± 73,5 ± 4,6 | ± 42,6 ± 3,4 | ± 21,7 ± 2,1 | ± 14,3 ± 1,0 | ± 11,6 ± 1,0 | ± 7,1 ± 1,3 |
|--|------------|---------------|--------------|--------------|--------------|--------------|--------------|-------------|

## Charge Exchange Scattering

Arrangement for observing the charge exchange scattering is shown in Fig. 5. In order to eliminate the count from the elastically scattered pions the quadruple coincidences 1,2,3,4 were set in anticoincidence with counter 8 placed before counter 3. Gamma detection efficiency is increased by the lead converter 7,35 g/cm<sup>2</sup> thick, placed before the counter 3.

The magnitudes of the ratios of number of quadruple coincidences to that of double observed in one of the runs of observations are given in Table 6.

The differential cross sections have been calculated according to the formula

$$\left(\frac{d\sigma}{d\omega}\right)_{\pi \rightarrow \gamma} = \frac{(Q/D)_{\gamma \text{ with H}} - (Q/D)_{\gamma \text{ without H}}}{N \cdot \omega \cdot K \cdot \epsilon} \quad (10)$$

where  $N = 0,443 \cdot 10^{24}$  is the average number of hydrogen atoms per  $\text{cm}^2$ .  $\omega$  is the solid angle subtended by angular telescopes.  $K$  is a coefficient taking into account conventional corrections.  $\epsilon$  is the detection efficiency for  $\gamma$ -rays.

The determination of  $\gamma$ -ray detecting efficiency is known to be a very difficult task. We used the gamma detection efficiencies given in Anderson and coworkers paper [3] because our geometry was approximately the same as Anderson's. Errors in the determination of the gamma detection efficiency give the main contribution to the experimental errors.

The differential cross section in the center of mass system obtained after all the corrections have been made for  $\gamma$ -quanta from  $\pi^0$ -meson decay in the process(2) are given in Tables 7, 8 and in Fig. 6. and 7.

Table 7

 $E_{\pi^-} = 307 \pm 9$  MeV $\pi^- + p \rightarrow \pi^0 + n$ 

|                         |       |       |       |       |       |        |        |        |
|-------------------------|-------|-------|-------|-------|-------|--------|--------|--------|
| The Angle in the c.m.s. | 20,5° | 40,5° | 59,2° | 76,8° | 98,0° | 128,1° | 146,4° | 159,4° |
|                         | 0,61  | 0,61  | 0,60  | 0,60  | 0,59  | 0,58   | 0,57   | 0,57   |

Differential cross section for  $\chi$ -quanta from meson decay in  $10^{-27}$  cm<sup>2</sup>/sterad

|       |        |        |        |        |        |        |        |        |
|-------|--------|--------|--------|--------|--------|--------|--------|--------|
| 9,8 ± | 8,46 ± | 4,05 ± | 2,24 ± | 1,50 ± | 1,40 ± | 1,32 ± | 1,32 ± | 1,32 ± |
| ± 2,0 | ± 1,74 | ± 0,83 | ± 0,46 | ± 0,31 | ± 0,31 | ± 0,30 | ± 0,30 | ± 0,29 |

Table 8

 $E_{\pi^-} = 333 \pm 9$  MeV $\pi^- + p \rightarrow \pi^0 + n$ 

|                         |       |       |       |       |       |        |        |        |
|-------------------------|-------|-------|-------|-------|-------|--------|--------|--------|
| The angle in the c.m.s. | 20,8° | 41,0° | 60,0° | 77,7° | 99,0° | 128,8° | 146,9° | 159,7° |
|                         | 0,62  | 0,61  | 0,61  | 0,60  | 0,60  | 0,59   | 0,58   | 0,57   |

Differential cross section for  $\chi$ -quanta from  $\pi^-$  meson decay in  $10^{-27}$  cm<sup>2</sup>/sterad.

|        |        |        |        |        |        |        |        |        |
|--------|--------|--------|--------|--------|--------|--------|--------|--------|
| 6,52 ± | 6,31 ± | 3,72 ± | 2,36 ± | 1,55 ± | 0,95 ± | 1,29 ± | 1,20 ± | 1,20 ± |
| ± 1,37 | ± 1,30 | ± 0,77 | ± 0,50 | ± 0,36 | ± 0,23 | ± 0,31 | ± 0,24 | ± 0,24 |

If we express the dependence of differential cross section on the scattering angle in the center of mass system in the form of (7) and (8), we obtain the coefficients given in Tables 9 and 10. The corresponding values of M are given in the same way.

Table 9

$E_{\pi} = 307 \text{ MeV}$

| $A_{\gamma}$    | $B_{\gamma}$    | $C_{\gamma}$    | $D_{\gamma}$ | $E_{\gamma}$ | M    |
|-----------------|-----------------|-----------------|--------------|--------------|------|
| $2,92 \pm 0,25$ | $3,30 \pm 0,53$ | $2,09 \pm 0,48$ | -            | -            | 6,29 |

Table 10

$E_{\pi} = 333 \text{ MeV}$

| $A_{\gamma}$    | $B_{\gamma}$    | $C_{\gamma}$    | $D_{\gamma}$    | $E_{\gamma}$     | M    |
|-----------------|-----------------|-----------------|-----------------|------------------|------|
| $2,64 \pm 0,22$ | $2,89 \pm 0,45$ | $1,55 \pm 0,40$ | -               | -                | 1,51 |
| $2,66 \pm 0,22$ | $2,95 \pm 0,46$ | $1,71 \pm 0,54$ | $0,18 \pm 0,63$ | $-0,04 \pm 0,54$ | 1,27 |

Just as in the case of elastic scattering, on the basis of the  $\gamma$ -quanta angular distribution form, one cannot draw a definite conclusion about the necessity of taking into account D-waves.

From the coefficients of expression (7) (as well as (8)) for the  $\gamma$ -quanta angular distribution it is easy to obtain the corresponding coefficients for  $\pi^0$ -meson angular distribution:

for  $E_{\pi} = 307 \text{ MeV}$   $A_0 = 1,46 \pm 0,12$ ;  $B_0 = 2,10 \pm 0,34$ ;  $C_0 = 1,78 \pm 0,40$

for  $E_{\pi} = 333 \text{ MeV}$   $A_0 = 1,32 \pm 0,11$ ;  $B_0 = 1,80 \pm 0,27$ ;  $C_0 = 1,27 \pm 0,33$

From these the integral cross section of the process (2) turns out to be equal:

for 307 MeV  $\sigma_{\pi^-\pi^0} = (8,4 \pm 1,6) \cdot 10^{-27} \text{ cm}^2$

for 333 MeV  $\sigma_{\pi^-\pi^0} = (16,6 \pm 1,4) \cdot 10^{-27} \text{ cm}^2$

The total cross section of  $\pi^-$ -meson interaction with hydrogen obtained from the angular distributions of elastic and charge exchange scattering if take into account the meson-meson production is

for 307 MeV  $\sigma_t = (30,2 \pm 1,8) \cdot 10^{-27} \text{ cm}^2$

for 333 MeV  $\sigma_t = (28,8 \pm 1,8) \cdot 10^{-27} \text{ cm}^2$

The total cross sections determined by a transmission experiments<sup>[4]</sup> are equal

for 307 MeV  $\sigma_t = (31,6 \pm 1,6) \cdot 10^{-27} \text{ cm}^2$  (interpolated value)  
(~~interpolated~~)

for 333 MeV  $\sigma_t = (25,7 \pm 1,0) \cdot 10^{-27} \text{ cm}^2$  ~~value~~

Phase shift analysis

There has been made a preliminary phase shift analysis of the data on  $\pi^-$ -meson elastic scattering at 307 MeV. It was supposed that only S and P waves participate in scattering and that the angular distribution of elastically scattered  $\pi^-$ -mesons at ~300 MeV is determined through phase shifts by the same equations as in the absence of inelastic processes. The phase shifts determining the interactions in S,  $P_{1/2}$  and  $P_{3/2}$  states with the isotopic spin 3/2 are denoted respectively  $\alpha_{31}, \alpha_{31}$  and  $\alpha_{33}$ . The values of these phase shifts  $\alpha_{31} = -23,2^\circ$ ,  $\alpha_{31} = -8,4^\circ$ ,  $\alpha_{33} = 133,2^\circ$  were taken from paper<sup>[5]</sup>. The phase shifts determining the interactions in S,  $P_{1/2}$  and  $P_{3/2}$  states with the isotopic spin 1/2 are denoted respectively  $\alpha_{11}, \alpha_{11}$  and  $\alpha_{13}$ . There was found four sets of phase shifts which give the

the minimum value of the weighted least squares sum  $M = \sum_{i=1}^7 (\Delta_i / \epsilon_i)^2$  where  $\Delta_i$  is the deviation of the differential cross section calculated from phase shifts at the given angle from the experimental one,  $\epsilon_i$  - the experimental error in the measured differential cross section. The obtained phase shifts and the corresponding magnitude  $M$  are given in Table II.

Table II

$E_{\pi\pi} = 307 \text{ MeV}$

| $\alpha_1$   | $\alpha_{11}$ | $\alpha_{13}$ | $M$ |
|--------------|---------------|---------------|-----|
| $5^\circ$    | $8^\circ$     | $-8,2^\circ$  | 1,4 |
| $1,5^\circ$  | $-22^\circ$   | $18^\circ$    | 1,5 |
| $15^\circ$   | $-19,5^\circ$ | $19,5^\circ$  | 1,3 |
| $11,8^\circ$ | $35,5^\circ$  | $70^\circ$    | 1,3 |

It is worth noting that neither of these sets of phases describe satisfactorily  $\gamma$ -quanta angular distribution from  $\pi^0$ -meson decay. This can be seen from Fig. 8.

At present there is in progress an electronic computer calculation of the phase shifts for  $\pi^+$ -meson<sup>151</sup> and  $\pi^-$ -meson [present work] scattering at the incident energy 307 MeV. We tried to fit 25 experimental data (23 differential cross sections and 2 total cross sections) with phase shifts which take into account either S,P,D or S,P waves. Four sets of phase shifts earlier obtained in the preliminary analysis were taken as input ones. It was supposed that the ~~input~~ values of phase shifts of D-waves are in absolute value less than 20.

Preliminary results are given below:

1. For S,P analysis the best set of phase shifts gives the weighted least squares sum M equal about 35 when the expected value is 19. In other words it seems that at energy 307 MeV it is necessary to take into account D-waves. The set is:

$$\alpha_3 = -2.5^\circ, \alpha_{31} = -10^\circ, \alpha_{33} = 133^\circ, \alpha_1 = 14^\circ, \alpha_{11} = 10^\circ, \alpha_{13} = -7^\circ.$$

2. For S,P, D analysis up to now we obtained only one set of phase shifts which gives - small enough value of M (about 17 when its expected value is 15):

$$\alpha_3 = -12^\circ, \alpha_{31} = -4.5^\circ, \alpha_{33} = 133.5^\circ, \delta_{33} = 8^\circ, \delta_{35} = -11^\circ$$
$$\alpha_1 = 16^\circ, \alpha_{11} = 16^\circ, \alpha_{13} = -3.5^\circ, \delta_{13} = 2.5^\circ, \delta_{15} = 5.5^\circ$$

Here  $\delta_j$  are the phase shifts for D-waves.

It is worth noting that the phase shifts for isotopic spin 3/2 in this set are close to the ones found by Mukhin and Pontecorvo<sup>151</sup> who investigated only positive pion scattering.

There is also one set of phase shifts which gives value M=24:

$$\alpha_3 = -19.3^\circ, \alpha_{31} = -9.1^\circ, \alpha_{33} = 132.7^\circ, \delta_{33} = 4.4^\circ, \delta_{35} = -6.6^\circ$$
$$\alpha_1 = -3.4^\circ, \alpha_{11} = -19.1^\circ, \alpha_{13} = 12.1^\circ, \delta_{13} = 4.4^\circ, \delta_{15} = 5.1^\circ$$

The other sets do not fit the experimental results (M > 30).

Additional calculations are in progress.



Constant of Meson-Nucleon Interaction  $f^2$  under  
Assumption of only S and P Wave contribution

From the measurements of  $\pi^-$ -meson elastic scattering one can get in principle some information of the value of the coupling constant of the meson nucleon interaction  $f$ . It is known that the energy dependence of the real part of the  $\pi^-$ -meson forward scattering amplitude  $D(0)$  can be obtained from dispersion relations<sup>3/</sup>. The behaviour of the curve depends on the value  $f^2$ . J. Puppi and A. Shangellini &/ called attention to the fact that in order to obtain a satisfactory agreement of such a curve with experimental data at the energy of  $\pi^-$ -mesons less than 180 MeV one must accept the value  $f^2 \sim 0,04$ . The data at the energies of  $\pi^-$ -mesons  $\sim 220$  MeV (as well as for  $\pi^+$ -mesons at the energies up to 400 MeV) are in agreement with the curve obtained if  $f^2 \sim 0,08 - 0,1$ . If we express  $D(0)$  through the coefficients of sum (7) and the total cross section of  $\pi^-$ -meson interaction with hydrogen  $\sigma_t$  then we obtain

$$D_-(0) \sqrt{(A_- + B_- + C_-) - \left(\frac{k\sigma_t}{4\pi}\right)^2} \quad (II)$$

where  $K$  - the wave number of a  $\pi$ -meson. Here it is assumed that only  $S, P$  waves contribute to scattering. The magnitudes  $D_-(0)$  thus calculated are equal in the centre of mass system

for 307 Mev  $D_-(0) = (-0,23 \pm 0,04) \times 10^{-13}$  cm

for 333 Mev  $D_-(0) = (-0,21 \pm 0,04) \times 10^{-13}$  cm.

The sign of  $D(0)$  was obtained on the basis preliminary  $S, P$  analysis. Such values  $D_-(0)$  (Fig. 9) are in satisfactory agreement with the magnitude  $f^2 = 0,08 - 0,1$ . This can be seen from the fig. 9 where the curve is taken from the paper of Puppi and Stanhellini(7).

It is necessary to note that the differential cross sections for the forward scattering obtained in our experiments both for elastic and charge exchange scattering are in good agreement with the curves calculated by Shernchaimex<sup>8/</sup> on the basis of dispersion relations at  $f^2 = 0,08$ . Such a curve for charge exchange scattering and the corresponding values obtained from the experiment are given in Fig. 10 as an example.

Of course if  $D$ -Waves really contribute to scattering we cannot make a priori conclusion that the value of  $f^2$  is equal 0,08.

Meson Production by  $\pi^-$  Mesons on Hydrogen in the Energy

Region of 300-370 MeV

A. Measurements and corrections.

The arrangement for observing the pions produced in pion-proton collisions is given in Fig. 11. Charged mesons produced in processes (3) and (4) and flying at the angle of  $80^\circ$  in the laboratory system were detected in the experiment. Such mesons give rise to quadruple coincidences in counters N 1,2,3 and 4. Of course mesons elastically scattered on hydrogen will also give rise to quadruple coincidences in counters N 1,2,3 and 4 and in considerably greater number. To exclude the counting of elastically scattered mesons the coincidences of counters N 1,2,3,4 were put in anticoincidences with counter 8 (Fig. 13 and 4) which was placed at the recoil proton angle for elastic scattering ( $37,5^\circ - 38^\circ$ ). Thus, only such quadruple coincidences of counters N 1, 2,3,4 which were not accompanied by the passage of a charged particle through counter 8 have been detected. These events are further called coincidences of type Q.

Not only mesons produced on hydrogen may give rise to such coincidences. Events of such type are possible also:

- a) when the recoil proton from process (1) is scattered on hydrogen or on the target walls and does not fall upon counter 8 while the corresponding  $\pi^-$ -meson is traversing the telescope of counters 3 and 4;
- b) in the double scattering by hydrogen and by the target walls of  $\pi^-$ -mesons, originally elastically scattered on hydrogen at the angle different from  $80^\circ$ ;
- c) when  $\gamma$ -quanta from the process (2) are converted in the target walls and in counter 3;
- d) when  $\pi^-$ -mesons from the process (2) decay (in 1,6% cases<sup>9/</sup>) according to the scheme  $\pi^- \rightarrow \gamma + e^+ + e^-$  and electrons are incident on the telescope 3,4;
- e) in the  $\pi^-$ -meson radiative process.

The coincidences of the type Q occur also due to the inefficiency of anticoincidence circuit. The correction which takes into account this inefficiency of anticoincidence circuits does not exceed 0,1% of the magnitude of the elastic scattering cross section. It was ~1% of the observed value of meson production mesons of 307 MeV.

PION PRODUCTY

| The energy of $\pi^-$ meson beam in MeV | The number of the coincidences 1,2,3,4-7,8 for $10^6$ counts of the monitor |                  |                 | The effect of $Pb_{66}$ for $10^6$ counts of the monitor (the difference with and without hydrogen) | The elastic scattering effect for $10^6$ counts of the monitor (the difference with and without hydrogen) | The coincidence with $\pi^-$ count monitor |
|---|---|------------------|-----------------|---|---|--|
|   | With hydrogen   | without hydrogen | net (averaged)  |   |   |  |
|   |   |                  | <u>Q</u>        |   |   |  |
| 250                                     | 8,97 $\pm$ 0,75   | 7,43 $\pm$ 0,52  | 1,73 $\pm$ 0,6  | 23,2 $\pm$ 2,1  | 9,83 $\pm$ 0,47   | 1,31 $\pm$ 0                               |
|   | 11,86 $\pm$ 0,6   | 9,99 $\pm$ 0,53  |                 |   |   |  |
| 307                                     | 10,17 $\pm$ 0,32  | 8,33 $\pm$ 0,26  | 1,84 $\pm$ 0,41 | 14,7 $\pm$ 1,7  | 8,5 $\pm$ 0,32  | 0,81 $\pm$ 0                               |
| 333                                     | 10,27 $\pm$ 0,37  | 7,50 $\pm$ 0,36  | 2,70 $\pm$ 0,48 | 14,3 $\pm$ 1,6  | 8,44 $\pm$ 0,32   | 0,79 $\pm$ 0                               |
|   | 16,4 $\pm$ 0,9  | 14,1 $\pm$ 0,8   |                 |   |   |  |
| 370                                     | 10,89 $\pm$ 0,67  | 8,60 $\pm$ 0,44  | 4,13 $\pm$ 0,45 | 11,2 $\pm$ 1,9  | 8,01 $\pm$ 0,32   | 0,62 $\pm$ 0                               |
|   | 11,51 $\pm$ 0,59  | 6,90 $\pm$ 0,53  |                 |   |   |  |
|   | 10,86 $\pm$ 0,55  | 7,37 $\pm$ 0,55  |                 |   |   |  |

SECTION BY  $\pi^-$  - MESONS ON HYDROGEN

Table 12

| The correction<br>deducted<br>from the<br>total number of<br>counts of the<br>monitor) | The<br>correction<br>connected<br>with<br>elastic<br>scattering<br>(for $10^6$<br>counts of<br>the monitor) | The num-<br>ber of<br>the Q-<br>type<br>coinciden-<br>ces cau-<br>sed by the<br>produced<br>mesons $\pi^0$<br>(for $10^6$<br>counts of<br>the monitor)<br><u>Q prod</u> | The de-<br>tected<br>share<br>of the<br>produced<br>pions at<br>the ener-<br>getic<br>spectrum<br>of the tra-<br>pezium farm<br><u><math>\epsilon</math></u> | The<br>"con-<br>ven-<br>tio-<br>nal"<br>cor-<br>rec-<br>tions<br><u>f</u> | The<br>diffe-<br>rential<br>cross<br>section<br>for the<br>product-<br>ion of<br>charged<br>meson<br>$f \frac{d\sigma}{d\omega} / 10^6 \text{ c.m.}^2$<br>$= \frac{d\sigma}{d\omega} / 90^\circ \text{ Lab.}$<br>in $10^{27} \text{ cm}^2/\text{ster}$ | $2.6(3) +$<br>$+0.76(4) =$<br>$= 4.37 \frac{d\sigma}{d\omega}$<br>in $10^{27} \text{ cm}^2$ |
|--|---|---|--|---|--|---|
| $1 \pm 0,33$   | $0,32 \pm 0,15$   | $0,1 \pm 0,7$   | $0,44$<br><i>OKALD</i><br>0  | -   | -  | -   |
| $1 \pm 0,2$  | $0,26 \pm 0,13$   | $0,77 \pm 0,48$   | $0,44$   | $0,96$  | $0,099 \pm 0,062$  | $1,24 \pm 0,78$   |
| $1 \pm 0,2$  | $0,25 \pm 0,13$   | $1,66 \pm 0,54$   | $0,57$   | $0,95$  | $0,166 \pm 0,054$  | $2,09 \pm 0,68$   |
| $1 \pm 0,2$  | $0,24 \pm 0,12$   | $3,27 \pm 0,51$   | $0,67$   | $0,92$  | $0,287 \pm 0,047$  | $3,61 \pm 0,59$   |

To determine the correction connected with a), it is necessary to know the cross section of the process (1) at the given angle (the coincidences of the counters 1,2,3,4,8). The coincidences of the counters 1,2,3,4,8 have been recorded during all the time when  $\theta$  was measured. The number of the recoil protons scattered in hydrogen and in the target walls has been determined from the total cross sections of nucleon interaction with hydrogen and carbon<sup>10/</sup>. Multiple and single proton scattering on Coulomb field of nuclei has been also taken into account.

The precise determination of double scattering contribution is practically impossible. All the double scattered  $\pi^+$ -mesons were considered to be isotropically distributed in space in the first rough approximation. The total number of double scattered mesons has been determined from total cross sections of elastic meson scattering on hydrogen and elastic and inelastic scattering on carbon<sup>11,12/</sup>. The number of double scattered mesons thus obtained was 1,8% from that of elastically scattered mesons. This correction is  $\sim 15\%$  of the observed number of produced mesons for energies of 307 MeV and for greater energies still less.

To determine the corrections connected with the effects c) and d) one must know what number of  $\gamma$ -quanta traverses the counter 3. With this aim measurements have been made in which a lead converter 7,35 g/cm<sup>2</sup> thick was placed before the counter 3 to increase the efficiency of  $\gamma$ -quanta detecting from process (2). If we know the cross section of  $\gamma$ -quanta conversion in hydrogen, carbon and lead we can estimate the magnitude of the correction for  $\gamma$ -quanta conversion in the counter 3 and in the target walls. It was  $4 \pm 1,5\%$  of the lead effect.

The correction taking into account the  $\pi^-$ -meson scattering with radiation was not made. Apparently the cross section of this scattering has the magnitude ~~not~~ less than 1% of the cross section of elastic  $\pi^-$ -meson scattering on hydrogen<sup>13/</sup>. At the energy of 307 MeV it may be ~10% of the observed effect of meson production by mesons.

Besides the numerated specific corrections the "conventional" ones have been also made. They take into account such effects:

$\mu^-$ -meson contamination in the beam ( $5 \pm 1,5$ )%, counting losses in the scatez of the monitor (up to 6%),  $\pi^-$ -meson absorption in the target walls and in hydrogen,  $\pi^-$ -meson absorption in the counter 3,  $\pi^-$ -meson decay.

To determine the background from mesons scattered in the target walls and in the counters 2 and 7, which is not connected with hydrogen, as well as that of accidental coincidences measurements with empty target have been made. Measurements with delayed coincidences showed that the accidental coincidences in the major part were conditioned by  $\pi^-$ -meson traversing the counters I and 2, and by accidental passage of any charged particles through both counters 3 and 4 at once. To reduce the background of accidental coincidences the counter 7 in anticoincidences with the counters I and 2 (Fig. 10 and 4) was used, so that the coincidences of the type Q have been recorded only in case if  $\pi^-$ -meson from the beam has been scattered in the target. This made it possible to reduce the background of accidental coincidence ~20 times. An additional reduction of the background of accidental coincidences was achieved by placing an aluminium absorber  $5,4 \text{ g/cm}^2$  thick between the counters 3 and 4.



As the intensity of the synchrocyclotron's work did not change more than 10% relatively to the average level, the variations of the background of accidental coincidences did not exceed  $\pm 0,05$  counts per  $10^6$  counts of the monitor. At the energy of 307 MeV it was 7% of the number of detected "produced mesons".

### B. Results

The experimental values obtained at different energies and all the corrections are given in Table 12. As expected at the incident pion energy of 250 MeV the produced mesons fail to be detected. This is due to the fact that the produced  $\pi$ -meson under the conditions of our experiment must have a kinetic energy more than 42 MeV in the laboratory system in order to be detected. The high threshold was due to a considerable extent by a aluminium absorber placed between counters N 3 and 4. The influence of the aluminium absorber on the efficiency of meson detection with different energies has been studied experimentally.

The existence of energetic threshold for pion detection leads to the fact that a considerable part of mesons produced on hydrogen fails to be detected. In order to determine what part of the produced mesons is not detected it is necessary to know the energetic spectrum of the produced mesons. As the data about such a spectrum are absent, assumptions concerning its form should be made. If we assume that the energetic spectrum is symmetrical in the center of mass system with respect to the energy equal to one half of the maximum energy of the produced  $\pi$ -mesons, then it turns out that the recording efficiency (i.e. the fraction of the produced mesons which are recorded) does not very strongly depend on the form of the

spectrum. So at the energy of incident pions 307 MeV the detecting efficiency is 44,8% 43,4% 42,7% for rectangular, trapezium and triangular form of the energetic spectrum respectively. At the energy of 370 MeV the respective efficiencies are equal to 60,8% 67%, 69,7%. In Table 12 the efficiencies for trapezium spectrum are given.

The differential cross section for the production of charged meson at the angle of  $80^\circ$  in the laboratory system has been calculated by the formula:

$$\left(\frac{d\sigma}{d\omega}\right)_{\text{prod}} = \frac{Q_{\text{prod}}}{N \cdot \omega \cdot f \cdot \xi} \cdot 10^{-6} \quad (12)$$

where  $Q_{\text{prod}}$  - difference between the observed value of Q-type coincidences and the contribution of the effects a), b), c), d) for  $10^6$  counts of monitor scaler.

$N=0,443 \cdot 10^{24}$  is the average number of atoms of hydrogen per  $1 \text{ cm}^2$ ;

$\omega = 0,0417$  steradian - ~~see~~ is the solid angle subtended by the telescope consisting of counters 3 and 4.

$\xi$  - the recording efficiency of the produced  $\pi$ -mesons if the energetic spectrum of these mesons has the trapezium form;

$f$  - a coefficient, taking into account the conventional corrections.

The angle of  $80^\circ$  in the laboratory system corresponds to that of  $105-107^\circ$  in the center of mass system. The corresponding coefficient transforming cross sections from one system to another differs from unit by not more than 1% on the average.

The differential cross sections obtained at different energies for the production of charged meson at the angle of  $80^\circ$  in the laboratory system, or  $\sim 106^\circ$  in the center of mass system are given in Fig. 12. The differential cross section is seen to grow rapidly with

energy. At the energy of 307 MeV the measured cross section is ~60% of the differential cross section of elastic scattering.

It is of interest to make on the basis of the obtained differential cross section an approximate estimate of the magnitudes of the total cross sections for meson production by mesons on hydrogen. If we assume that the meson angular distribution in both processes (3) and (4) is isotropic and the mesons are not correlated, then the magnitude  $(\frac{d\sigma}{d\omega})_{\text{prod. } 4\pi}$  is the sum  $2\sigma_{(3)} + 0,7\sigma_{(4)}$  of the total cross sections of processes (3) and (4) (Table I). The coefficient 2 before  $\sigma_{(3)}$  arises because two charged mesons are obtained in process 3. The coefficient 0,7 before  $\sigma_{(4)}$  is connected with the fact that approximately 30% of the recoil protons from the process (4) may be incident on counter 8, reducing respectively the  $\pi^-$ -meson recording efficiency from the process (4).

Some theoretical papers has been recently published the results of which can be compared with the magnitudes of total cross sections obtained under the abovementioned assumptions. In a recent paper<sup>14</sup> the charge symmetrical pseudoscalar interaction has been considered using Tamm-Dankoff approximation, the amplitudes of all the states containing more than two meson having been neglected. According to this paper the contribution of meson production by mesons in the energy interval investigated is less than 1% of the magnitude of the elastic scattering. It is, at least, 10 times less than the obtained values. It is worth noting that the Tamm-Dankoff method gives the results which do not agree with the experiment also for usual  $\pi^-$ -meson scattering on protons.

The cross sections of the processes (3), (4) and (5) on the basis of Chew-Low theory have also been calculated recently (15).

The dependence of the sum  $2\sigma_{(3)} + 0,7\sigma_{(4)}$  on  $\pi^-$ -meson ener-

gy, which is obtained on the basis of the data of this work is given for comparison in Fig. 12 in the form of solid curve. From the methodical point of view the fact that there is no great discrepancy between the experimental data and that of work<sup>15/</sup> is of some interest.

### S u m m a r y

1. The differential cross sections of elastic and charge exchange  $\pi^-$ -meson scattering on hydrogen for energies of incident  $\pi^-$ -meson 307 and 333 MeV have been measured. (Fig. 8 and 9, Tables 2,3,7,8) Taken
2. From the obtained angular distributions it follows that the coupling constant of meson-nucleon interaction  $f^2$  has the value 0,08-0,1. This conclusion is valid only if it turns out that only S and P waves contribute to the scattering process.
3. On the basis of the form of the various angular distributions taken by themselves one cannot draw conclusions about the necessity of taking into account D-wave contribution  $\pi^-$ -meson scattering in hydrogen at the energy of 307 and 333 MeV. However, a preliminary phase shift analysis of the data on  $\pi^-$ -meson scattering on hydrogen at the energy of 308 MeV (25 data) points out that a SPD analysis is probable necessary.
4. The differential cross sections for the production of ~~processes~~ charged mesons at the angle of  $80^\circ$  in the laboratory system ( $105-107^\circ$  in the center of mass system) in the processes (3) and (4) are obtained. (Fig. 14, Table 12). It turns out that the differential cross sections are by no means small (at 370 MeV the inelastic cross section is about 60% of elastic cross section).

The authors express their gratitude to professor B.M. Pontecorvo for constant interest and assistance in the present research. and to H.N. Tentiukova for carrying out electronic computer calculation of the phase shifts.

R E F E R E N C E S

1. A.E. Ignatenko, V.V. Krivitsky, A.I. Mukhin, B.M. Pontecorvo, A.A. Reut, K.I. Tarakhanov. The Soviet Journal of Atomic Energy 5, 5 (1956)
2. S.M.Korenchenko and V.T. Zinov, JETP (in press)
3. H.L. Anderson and M. Glicksman, Phys. Rev. 100, 26 (1955);  
H.L. Anderson, W.C. Davidon, M. Glicksman and U.S. Kruse, Phys. Rev. 100, 279 (1955)
4. A.E. Ignatenko, A.I. Mukhin, E.B. Ozerov and B.M. Pontecorvo, Dokl. UUSR Acad. Sci. 103, 45 (1955)
5. A.I. Mukhin, B.M. Pontecorvo, JETP, 31 550 (1956)
6. H.L. Anderson, W.C. Davidon and U.S. Kruse, Phys. Rev. 100, 339 (1955)
7. G. Puppi and A. Stanghellini, Nuovo Cimento 5, 1305 (1957)
8. Sternhaimer, Sixth Annual Rochester Conference on High-Energy Nuclear Physics (Interscience Publishers, Inc. New York, 1956)
9. P. Lindenfeld, A. Sachs and J. Steinberger, Phys. Rev. 89, 531 (1953)
10. See for example, the survey by V.I. Goldansky, A.L. Lyubimov and B.M. Medvedev - Uspechy Fys. Nauk, 61, 341 (1956)
11. L.M. Barkov and B.A. Nikolsky, Uspechy fys. Nauk 61, 341 (1953)  
(Survey)
12. V.P. Dzhelepov, V.T. Ivanov, M. S. Kozodaev, V.T. Osipenkov, N.I. Petrov, V.A. Rusakov, JETP, 31, 925 (1956).
13. V. T. Soloviev, JETP, 29, 242 (1955)
14. M. Nelkin, Phys. Rev. 104, 1150 (1956)
15. J. Franclin, Phys. Rev. 105, 1101 (1957)

.....

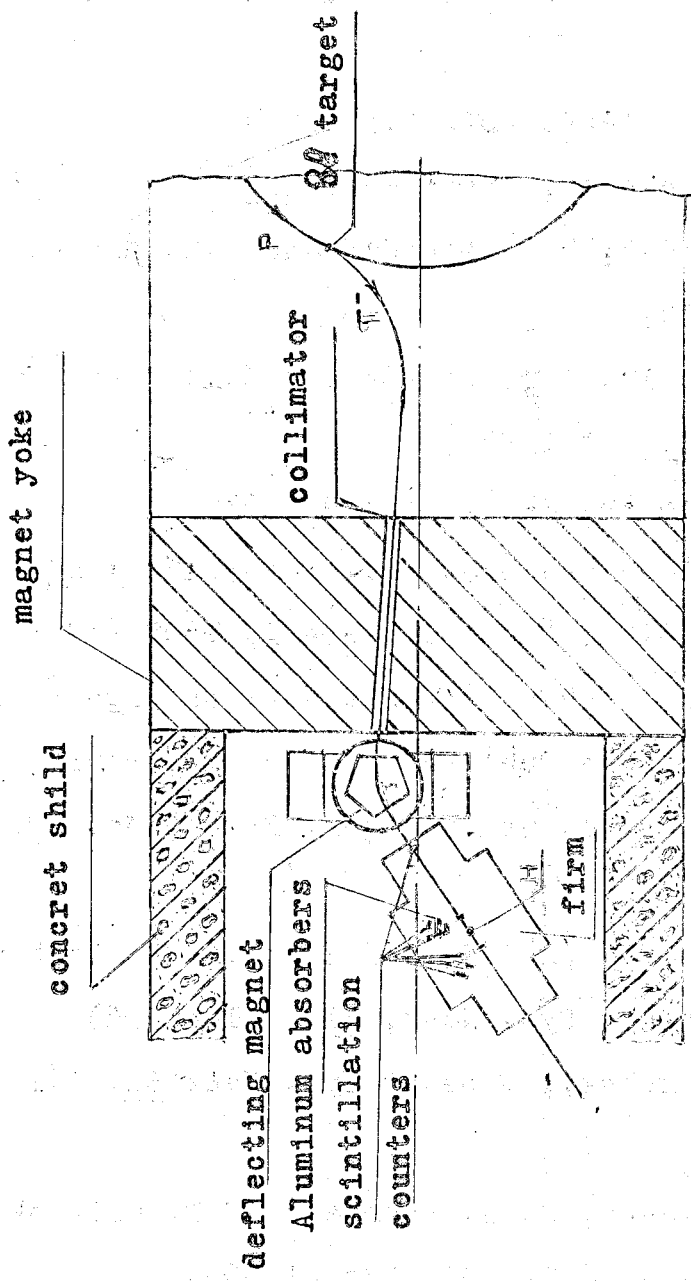


Fig. 1.

General arrangement for observing  $\pi$ -meson interaction with proton.

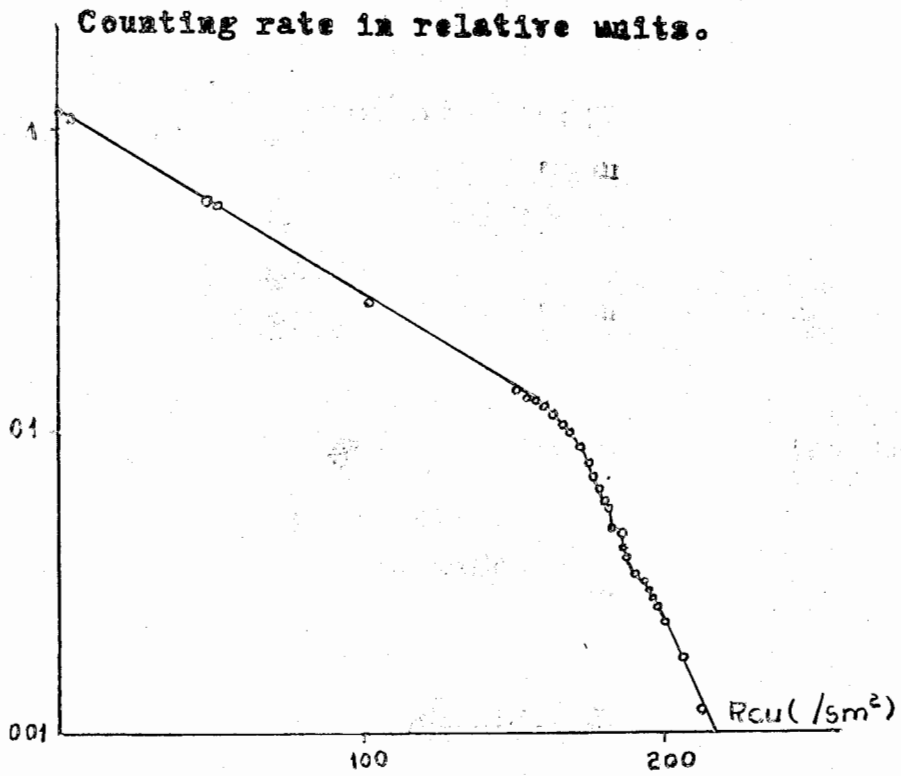


Fig. 2.

Range  $\gamma$  curve in copper ( $E_{\beta_{max}} = 307$  MeV)

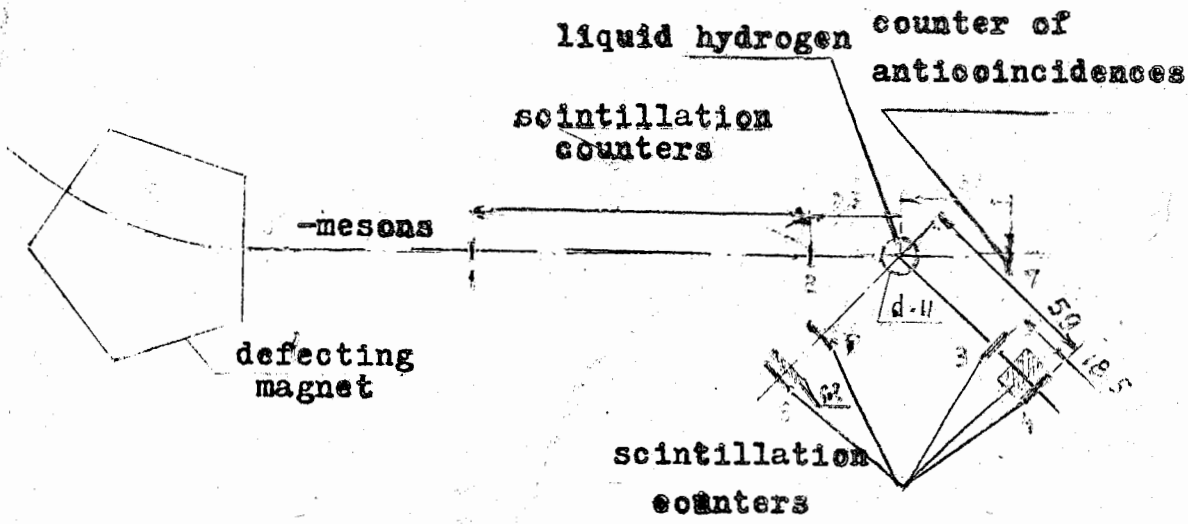


Fig. 3.

Arrangement for observing the elastic scattering of negative pions in hydrogen.



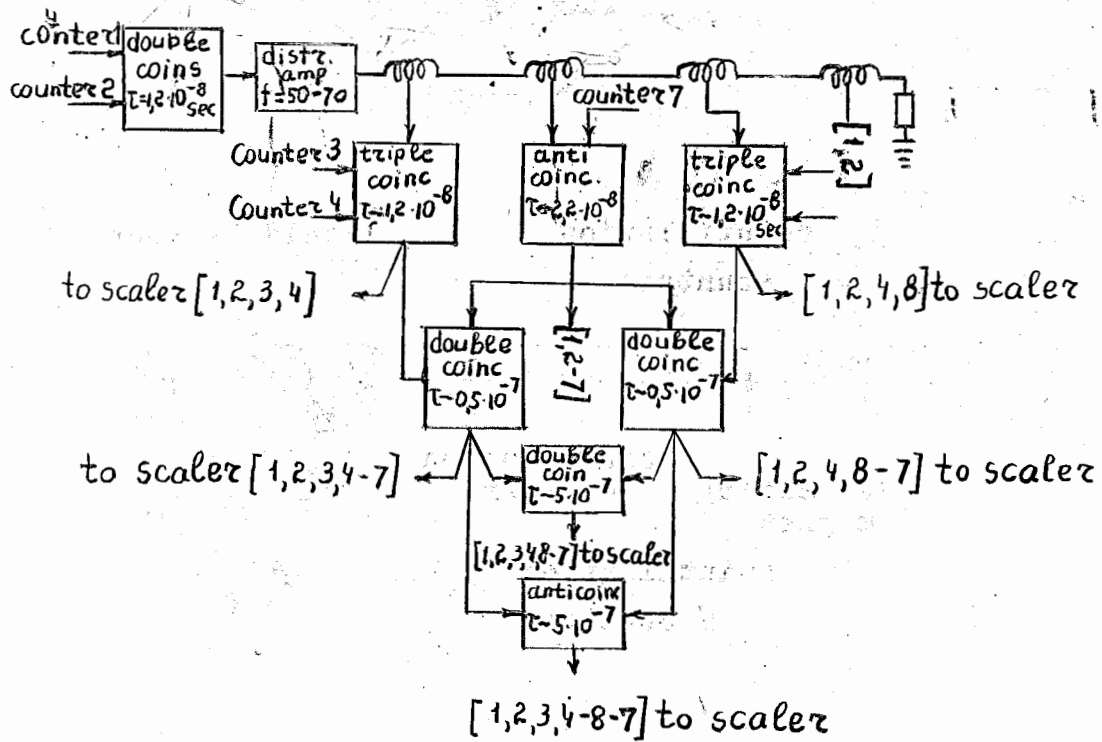


Fig. 4

Block - diagram of electronic equipment.

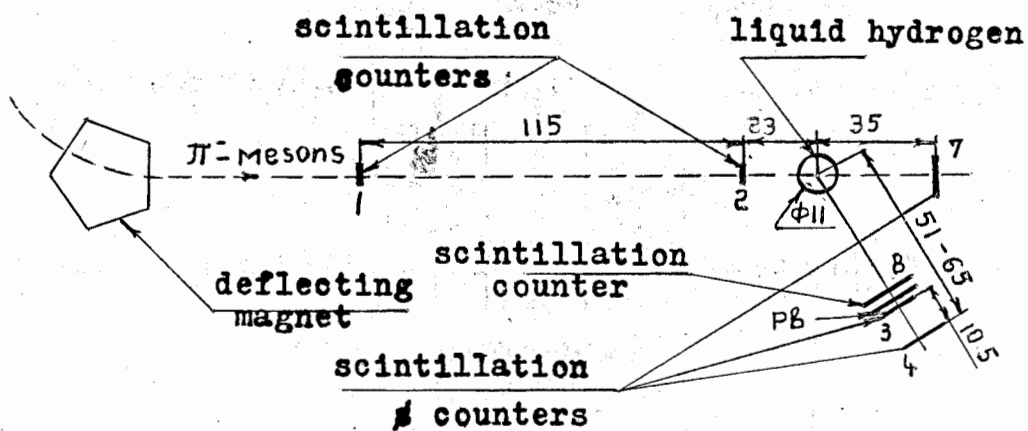


Fig. 5.

Arrangement for observing the charge exchange scattering of negative pions in hydrogen.

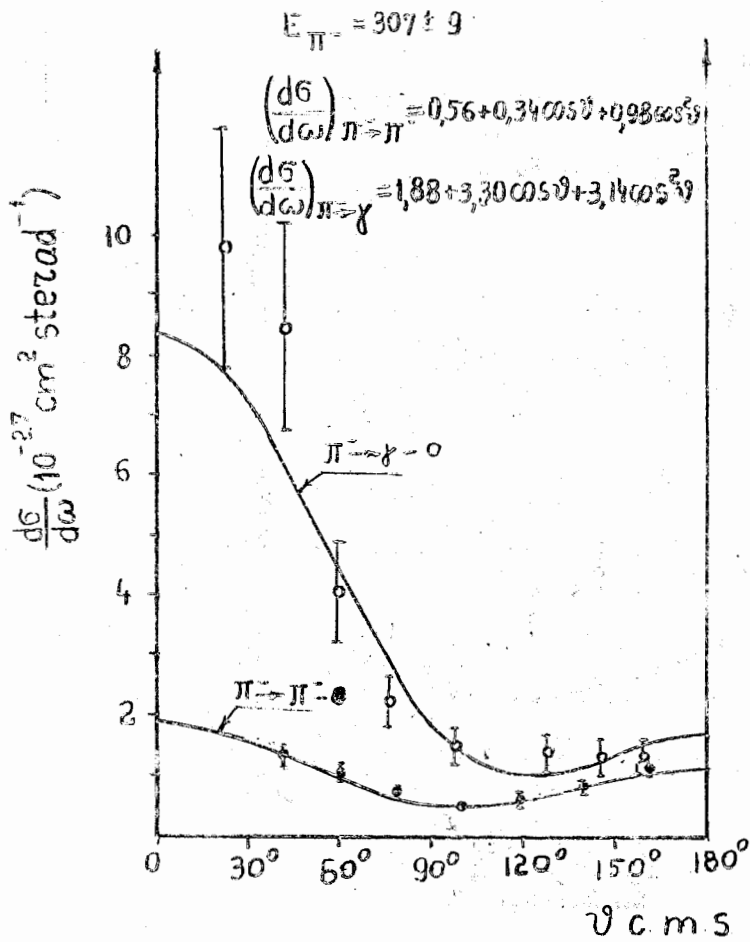


Fig. 6.

Differential cross sections of elastic and charge exchange scattering of negative pions in hydrogen at the energy. 307 Mev

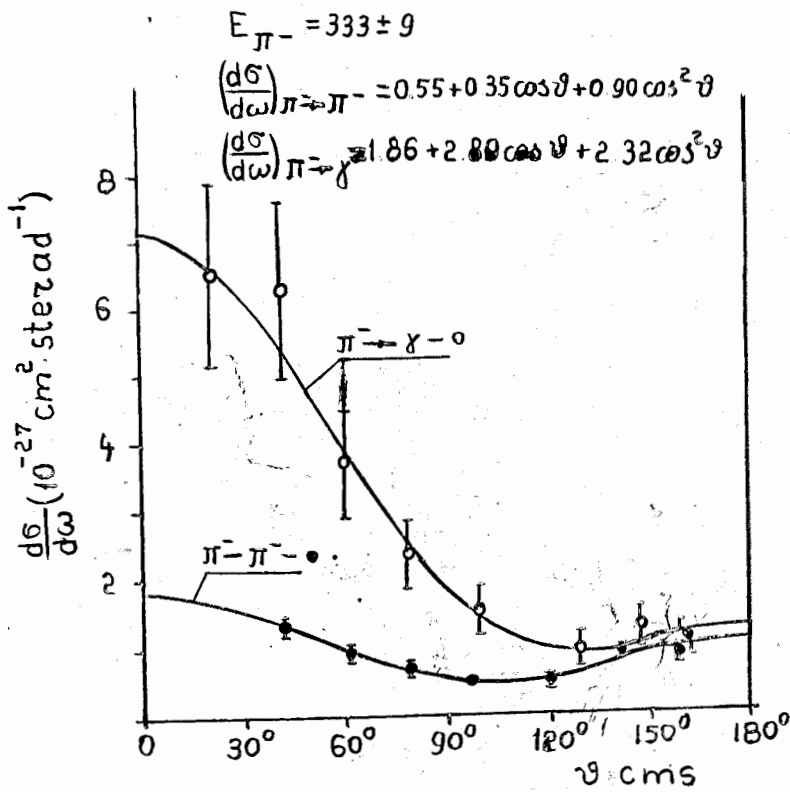


Fig. 7.

Differential cross sections of elastic and charge exchange scattering of negative pions in hydrogen at the energy 333 MeV.

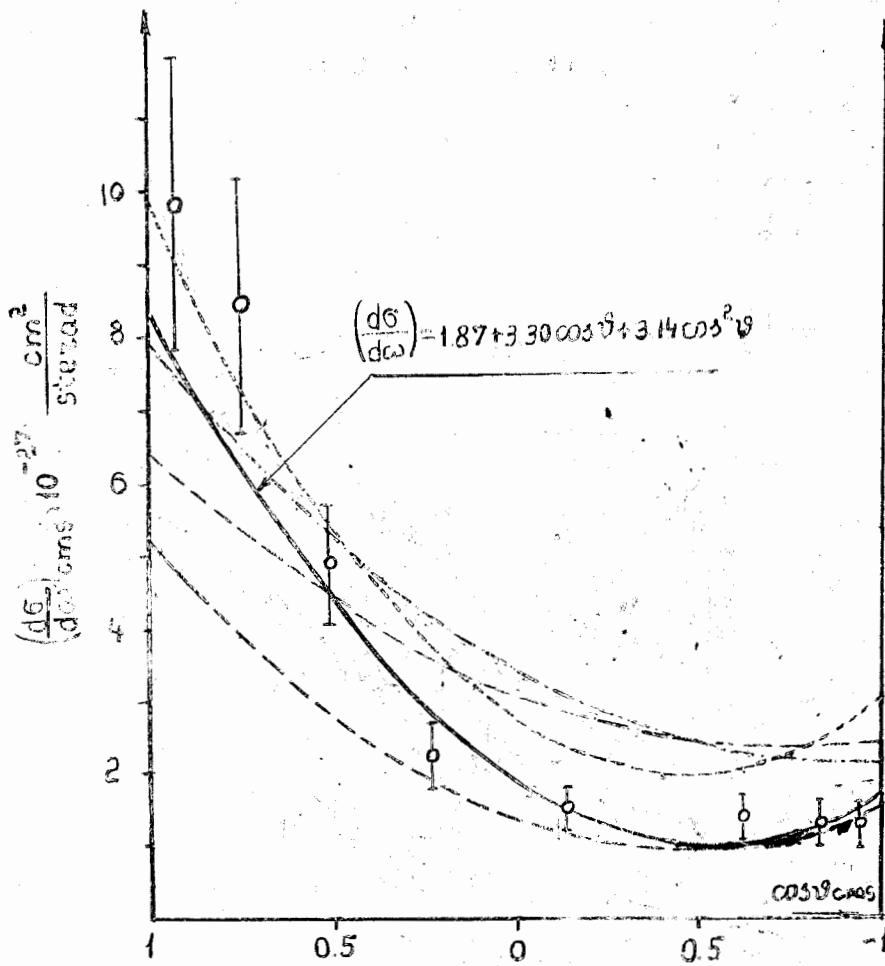


Fig. 8.

Angular distribution of  $\gamma$ -rays from  $\pi^0$ -meson decay ( $E_{n\pi} = 307$  MeV). Dotted curves calculated from S, P preliminary phase shifts.

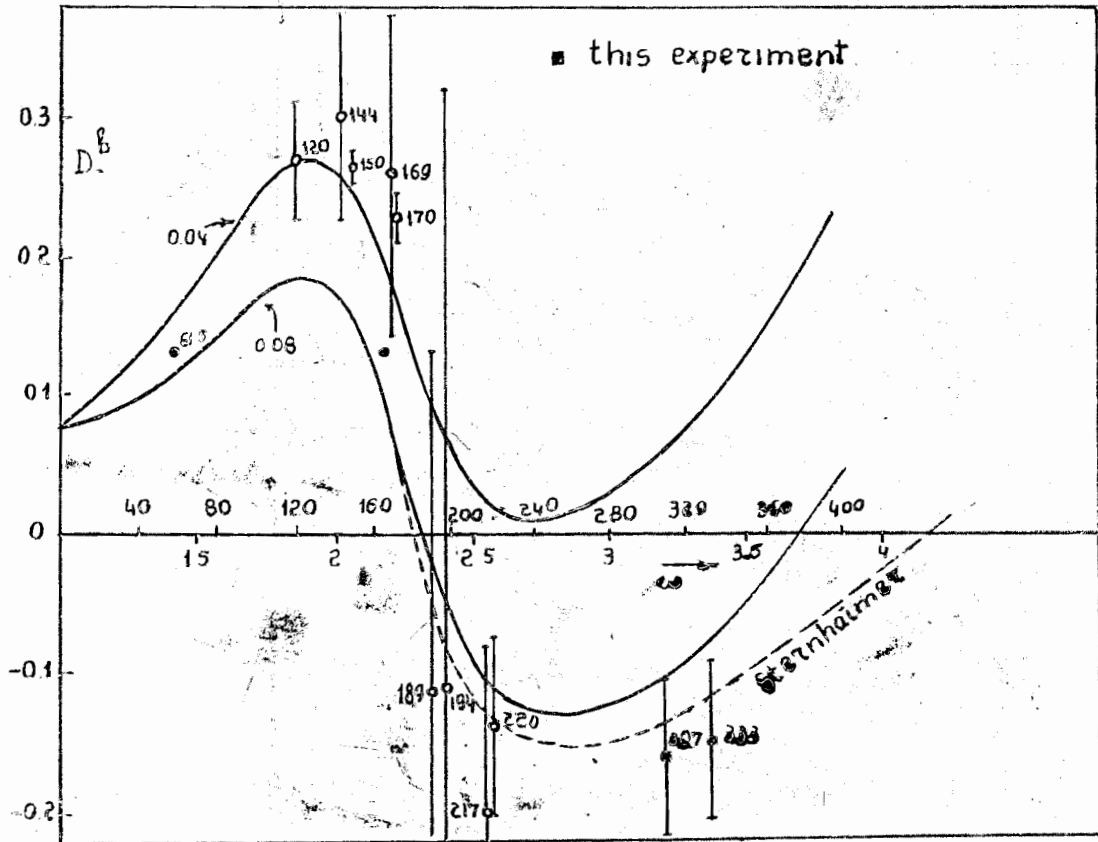


Fig. 9.

Energy dependence of the real part  $\pi^- + p$  forward scattering amplitude  $|f|$ .

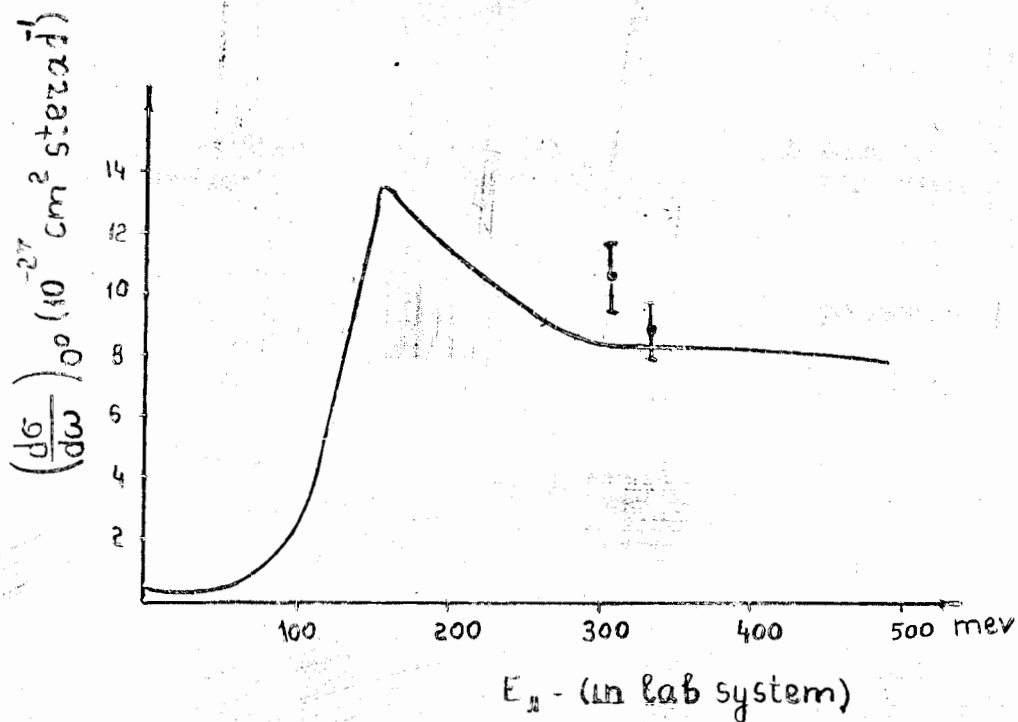


Fig. 10.

Calculated energy dependence of the differential cross section at  $0^\circ$  for charge exchange negative pion scattering ( $f^2 = 0,08$ ) |<sup>8</sup>|.

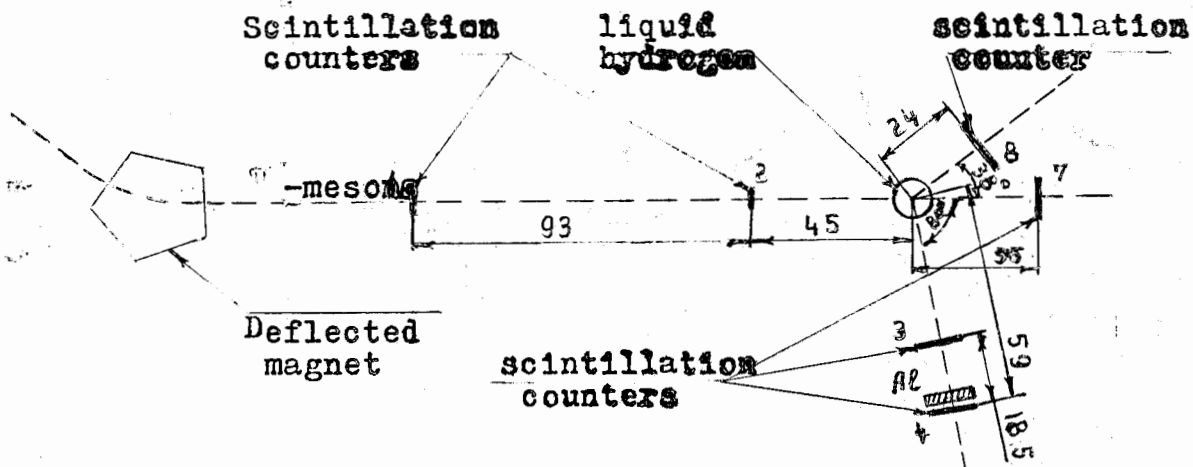


Fig. 11.

Arrangement for observing charged pion production in pion-proton collisions



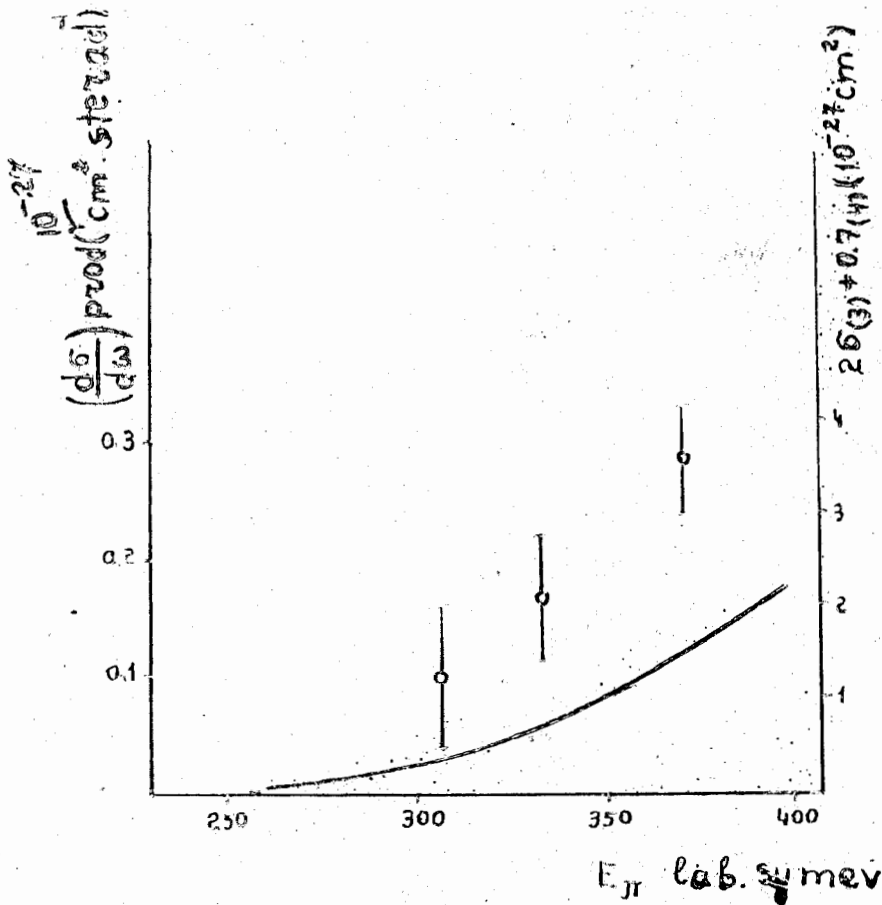


Fig. 12.

Differential cross sections of charged pion production at laboratory angle  $80^\circ$  ( $\sim 106$  e.m.) in pion-proton collisions. Solid curve obtained from Franklin's calculations [15].